Journal of Porous Materials (2020) 27:1735–1743
https://doi.org/10.1007/s10934-020-00949-2

The effect of mesoporous support on the catalytic performance of Pd nanoparticles in the hydrogenation of cyclopentene

Mhamed Benaissa[1,2] · Abdullah M. Alhanash[1] · Murad Eissa[1] · Ali Aldalbahi[3,4] · Shaykha Alzahly[3] · Mostafizur Rahaman[4] · Govindasami Periyasami[4] · Mohamed S. Hamdy[1]

Published online: 3 August 2020

Abstract
Here, a comparison between four mesoporous siliceous compounds is conducted to investigate the effect of support on formation and catalytic behavior of palladium (Pd) nanoparticles. The four investigated supports are: the commercially available MCM-41, SBA-15 and MCM-48, in addition to the home-made TUD-1 material. The same amount of Pd (Si/Pd = 200) was impregnated in the four mesoporous samples by using water as a solvent, and no further activation/reduction was performed. The obtained characterization data showed that SBA-15 accommodated the maximum amount of PdO nanoparticles that located inside its channels, while the maximum surface area after impregnation was obtained in MCM-48 sample. The four Pd samples was used to catalyze the solvent-free reduction of cyclopentene at room temperature by using 1 atm of hydrogen gas. Pd-TUD-1 exhibited the maximum activity with a total TOF of 4.83 s^{-1}, while the TOF of SBA-15 was 2.28 s^{-1}. The activity results clearly show the effect of the open three dimensional structure of TUD-1 in offering the maximum accessibility to and from Pd nanoparticles' active sites.

Keywords Mesoporous · TUD-1 · MCM-41 · SBA-15 · Palladium · Hydrogenation

1 Introduction

Hydrogenation reactions are classified as highly importance in the chemical industry's sector [1, 2]. The aim of this type of reaction is conversion of the unsaturated organic compounds to -partially or totally- saturated compounds [3]. Supported Noble metals such as Au [4], Pd [5], Rh [6], Pt [7], and Ru [8] and their complexes [9] represent the best catalysts for hydrogenation reactions and they have been used in petrochemical and pharmaceutical industries in spite of the higher cost of the production process. One of the strategies to minimize the overall cost of the hydrogenation process is the use of a good supporting material for the applied Noble metal nanoparticles [10]. The ideal support must facilitate the heterogeneous catalytic reaction process to reduce the reaction time and therefore increase the productivity and minimize the production costs. Several supports such as metal oxides [11], zeolites [12], clays [13], and MOF's [14, 15] were applied as a support in hydrogenation reactions, however, amongst the applied supports, mesoporous silica is a promising candidate in industrial processes to accommodate the Noble metal nanoparticles. Mesoporous silica is chemically stable, owns higher surface area and silica itself is abundant. Currently, several mesoporous materials are commercially available such as MCM-41, SBA-15, MCM-48, and HMS.

Several studies reported the use of mesoporous silica as a support of the metal active sites in hydrogenation reactions. MCM-48 was reported to accommodate Pd [16] nanoparticles, on the other hand, MCM-41 supported Pt [17], finally, SBA-15 was applied as a support for Rh [18] and Ru [19]. Hamdy and coworkers reported the use of TUD-1 mesoporous material as a support for Pd [20, 21] and Rh

✉ Mohamed S. Hamdy
m.s.hamdy@gmail.com

1 Catalysis Research group (CRG), Department of Chemistry, College of Science, King Khalid University, P.O. Box 9004, 61413 Abha, Saudi Arabia

2 Chemical Engineering Department, College of Engineering, University of Hail, P.O. Box 2440, Hail, Saudi Arabia

3 King Abdullah Institute for Nanotechnology, King Saud University, 11451 Riyadh, Saudi Arabia

4 Department of Chemistry, College of Science, King Saud University, 11451 Riyadh, Saudi Arabia

[22] in the hydrogenation of cyclooctadiene and cyclohexene, respectively.

The hydrogenation of cyclopentene to cyclopentane is an important industrial reaction. Industrially, cyclopentene is normally produced during the steam cracking of naphtha. Due to the limited use of cyclopentene and because it has only few applications, it used as a component of gasoline. Cyclopentane has several industrial applications, it is used in rubber adhesives and resins, and it is used in polyurethane foam manufacturing. One interesting application of cyclopentane that it can replace the hydrofluorocarbon compounds in refrigerators and freezers and minimize the environmental damage produced from the use of hydrofluorocarbon compounds. Therefore, the reduction of cyclopentene to cyclopentane can add a great value to the chemical industry.

In the current study, an attempt was carried out to design an active catalyst to catalyze the reduction of cyclopentene to cyclopentane. Four different mesoporous materials were applied to accommodate the same Pd loading, after characterization, the catalytic behavior of the four Pd catalysts was investigated in the reduction of cyclopentene at room temperature by using H_2 gas. The catalytic data as well as the recycling study of the catalyst of choice are reported and discussed.

2 Experimental

2.1 Pd catalysts reparation

The commercially available MCM-41, SBA-15 and MCM-48 were obtained from Sigma-Aldrich. TUD-1 was prepared as reported earlier in [23]. Pd nanoparticles were impregnated in the four mesoporous materials as following: 1 gram of the silica support was added to 100 ml of deionized H_2O and the calculated amount of palladium nitrate hexahydrate (98.0% Sigma Aldrich) was added to each suspension. The suspensions were kept for 24 h under vigorous stirring with a rate of 850 rpm, after that the solid powders were filtrated, and washed few times with deionized water, dried at 98 °C for 24 h and finally calcined at 450 °C for 4 h with a heating ramp of 5 °C/min. The four Pd catalysts were characterized as reported by the current research team in [22].

2.2 Catalytic activity study

A 300 ml Parr reactor was used to study the reduction of cyclopentene by using hydrogen gas as a reducing agent. The reaction was performed without the addition of any solvent. In a typical reaction, 0.25 g of Pd catalyst was carefully ground and sieved and then mixed in the reactor with 25 ml cyclopentene (≥ 99%, Sigma-Aldrich) to form a suspension. The suspension was vigorously stirred with a constant rate of 1000 rpm to reduce the external mass transfer limitation, if present. After closing the reactor carefully, it was degassed with nitrogen gas and finally pressurized to 1 atm with hydrogen gas (99%). After elapsing the reaction time, the reactor was flushed with nitrogen gas and finally a sample of 0.5 ml was sent to GC for analysis. The applied GC was SHIMADZU GC-17, and the applied capillary column was RTX-5, 30 m × 0.25 mm × 0.25 µm, finally, the applied detector was a flame ionization type (FID).

The conversion of cyclopentene (CPE) was calculated as following

$$\text{Conversion} = \frac{[CPE]_0 - [CPE]_t}{[CPE]_0} \times 100$$

where $[CPE]_o$ is the concentration of cyclopentene at zero time, $[CPE]_t$ is the concentration of cyclopentene at (t) time.

Moreover, the turnover frequency (TOF) was calculated as following

$$\text{TOF} = \frac{[CXE]_0 - [CXE]_t}{[Pd] \times time(s)}$$

where [Pd] is the Pd number of moles, while the time of reaction was calculated in seconds.

3 Results and discussion

3.1 Catalysts' characterization

The elemental analysis (which was performed by ICP) of the Pd% in the four investigated catalysts after synthesis is compared with the intended loading % in Fig. 1. Generally speaking, the Pd loading in the four samples is less than the intended loading, which means that not all the Pd amount presents in the solution was incorporated and/or bonded to the mesopores and/or silica surface, respectively. The percentage of Pd loss reached maximum in the case of MCM-48 where 23%, while SBA-15 exhibited the maximum loading where only 14% of Pd ions were not found in the final solid catalyst.

The N_2 physisorption analysis of the four samples (Fig. 1b) showed that the Pd-MCM-48 exhibited the highest surface area followed by Pd-MCM-41, while Pd-TUD-1 exhibited the minimum surface area. However, Pd-TUD-1 catalyst owned the wider pore size which is almost two times higher than the rest of the investigated catalysts. The texture properties of the four investigated catalysts are listed in Table 1.

XRD patterns of the four supports before and after Pd impregnation are plotted in Fig. 2. The entire mesoporous silica supports before and after Pd functionalization showed a broad peak between 20 and 30 2theta. This beak is

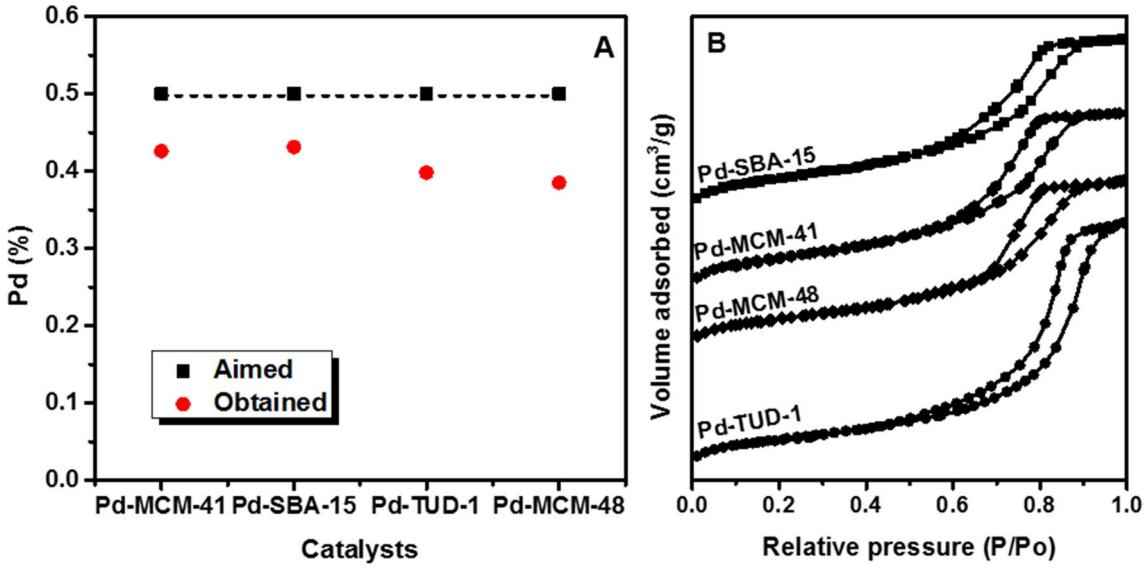

Fig. 1 **a** The aimed and the obtained Pd loading % in the four investigated catalysts. **b** The N_2 isotherms of the four investigated samples

Table 1 The elemental analysis and the texture properties of the four investigated catalysts

	Pd loading (%)		Texture properties		
	Synthesis	Product	Surface area m^2/g	Pore volume cm^3/g	Pore size nm
Pd-MCM-41	0.5	0.426	770.9	0.071	2.1
Pd-SBA-15	0.5	0.431	672.4	0.211	2.1
Pd-TUD-1	0.5	0.398	602.7	0.540	3.8
Pd-MCM-48	0.5	0.385	851.5	0.052	2.0

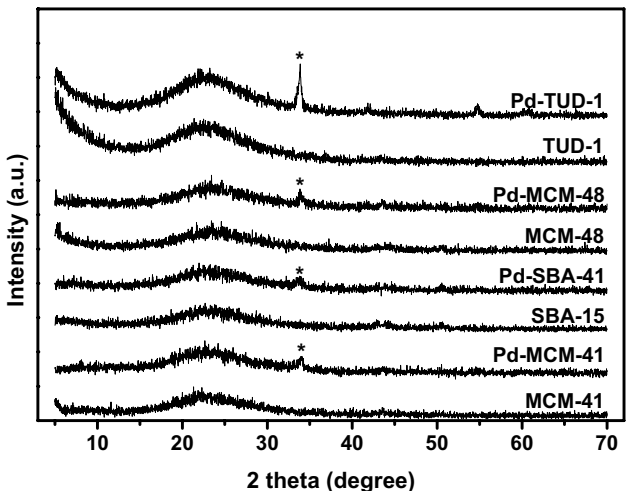

Fig. 2 The XRD patterns of the four mesoporous supports before and after Pd functionalization

indicated the amorphous silica matrix as reported by Adam et al. [24]. It is important to mention that neither the intensity nor the location of this beak changed after Pd impregnation as an indication of the morphology stability. Moreover, other peaks were detected in the impregnated samples at 33.7°, 54.5°, and 60.7° 2theta, which can be attributed to the planes of (101), (112), and (200) of palladium oxide, respectively. Moreover, the location of the observed peaks are perfectly matching the JCPDS card no. 43-1024 [25].

Moreover, the formation of PdO nanoparticles in the four investigated mesoporous silica materials was confirmed by using Raman spectroscopic technique (Fig. 3). The Raman spectra of the entire investigated Pd catalysts showed one intensive peak around 646 cm^{-1} which is characteristic to PdO phase as reported earlier by Forzatti et al. [26].

The surface morphology of the four investigated catalysts was investigated by scanning electron microscopy which coupled with EDX analysis. The SEM micrographs of the four catalysts are presented in Fig. 4a–d. The four catalytic samples exhibited four different morphology, i.e. Pd-MCM-41 and Pd-TUD-1 exhibited irregular-shape particles, Pd-SBA-15 exhibited a worm-like structure, and MCM-48 exhibited a spherical-like particles. Moreover, no new phase either crystalline or amorphous was detected, which agrees the total incorporation of PdO in the four investigated silica

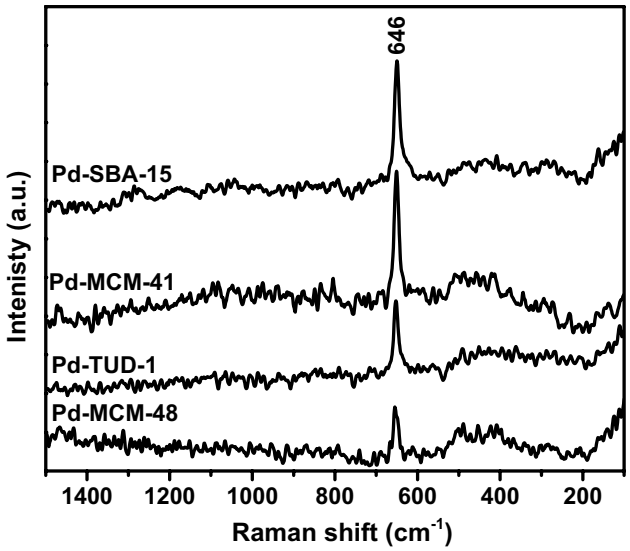

Fig. 3 The Raman spectra of the four Pd catalysts as collected at ambient conditions

matrices. The distribution of Pd was observed by mapping technique, it was found that Pd nanoparticles are highly distributed throughout the silica support in the four investigated catalysts.

The presence and the distribution of Pd nanoparticles inside the four investigated catalysts was investigated by using HR-TEM. The obtained micrographs (Fig. 5) showed that the majority of PdO nanoparticles are located inside the pores of the supported silica with a possible deposition (minor) in the case of MCM-48 and TUD-1. Moreover, no bulky crystalline phase of PdO could be observed. The obtained result showed clearly that PdO nanoparticles were able to form inside the pores of the different silica supports by using the applied synthesis method and by using only water as a solvent.

3.2 Catalytic performance

The catalytic performance of the four Pd catalysts in cyclopentene reduction by using hydrogen gas at room temperature is presented in Fig. 6. The reactions were performed for 45 min by using batch method. The obtained results showed that Pd-TUD-1 catalyzed the total conversion of cyclopentene to cyclopentane within the reaction time, in another word, Pd-TUD-1 exhibited the best activity amongst the four prepared catalysts. Moreover, Pd-SBA-15 catalyzed the conversion of 52.9% of cyclopentene, while, the conversion of cyclopentene over MCM-41 and MCM-48 was 41.6 and 37.4% respectively.

The calculated TOF, which was calculated based on the total amount of Pd active sites, showed that Pd-TUD-1 exhibited the maximum TOF of 4.83 s^{-1}, while Pd-MCM-48 showed the minimum TOF which was 1.74 s^{-1}. Generally speaking, the TOF of Pd-TUD-1 was almost 2–2.5 times higher than that of the other investigated catalysts (Fig. 7).

Because Pd-TUD-1 exhibited the best catalytic activity, it was chosen for further investigations, e.g. recycling

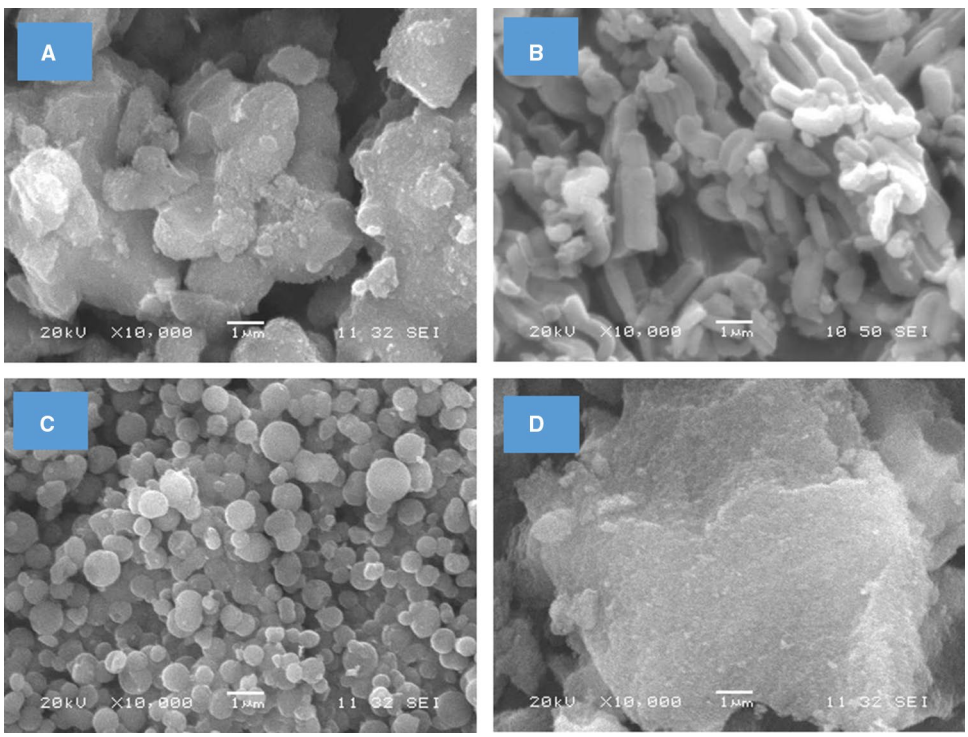

Fig. 4 The morphological structure of the four investigated catalysts as obtained from SEM micrographs of **a** Pd-MCM-41, **b** Pd-SBA-15, **c** Pd-MCM-48, and **d** Pd-TUD-1

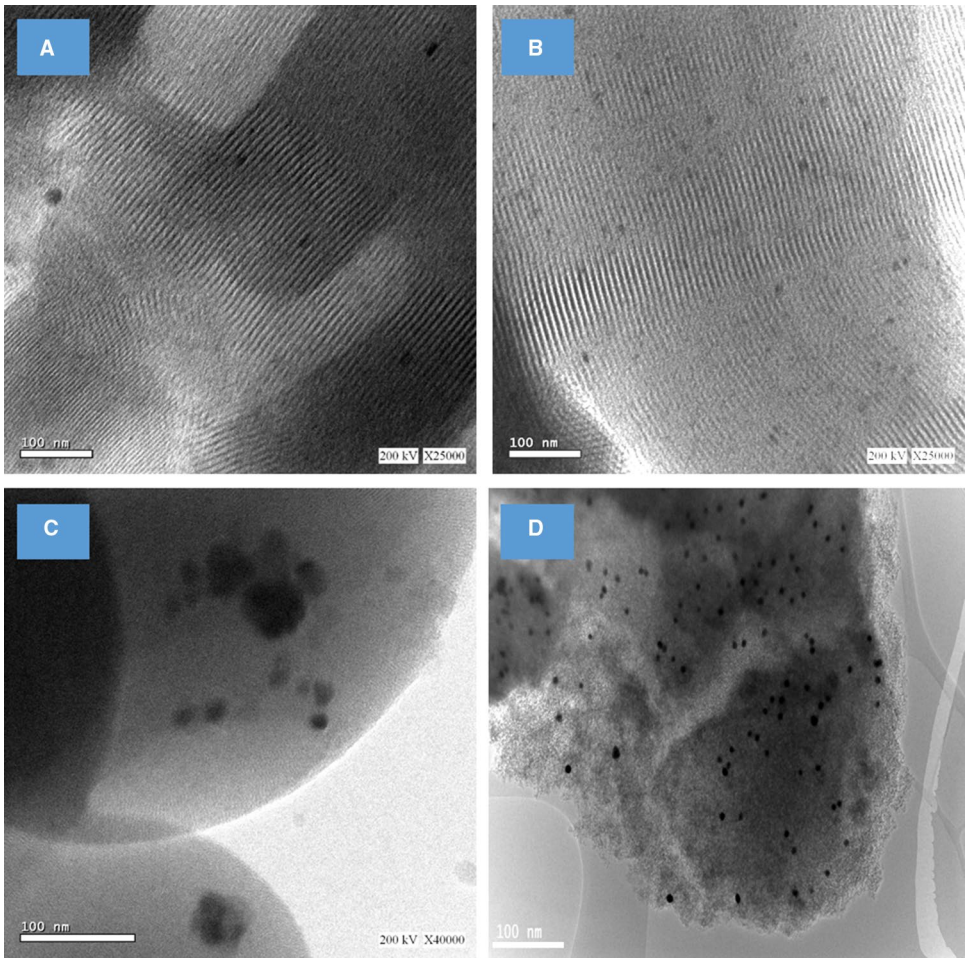

Fig. 5 HR-TEM micrographs of **a** Pd-MCM-41, **b** Pd-SBA-15, **c** Pd-MCM-48, and **d** Pd-TUD-1

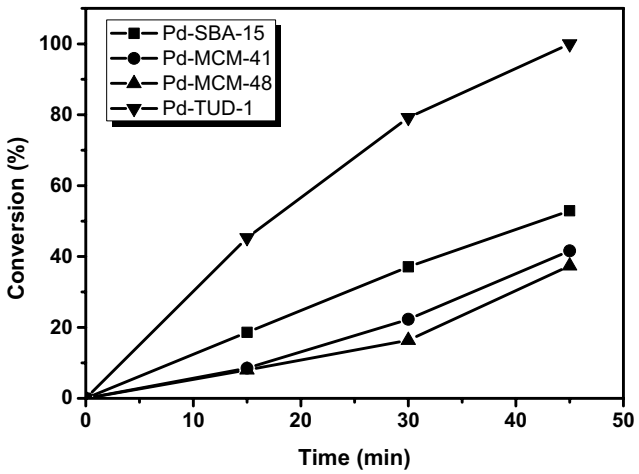

Fig. 6 The hydrogenation of cyclopentene over the four investigated catalysts as a function of reaction time

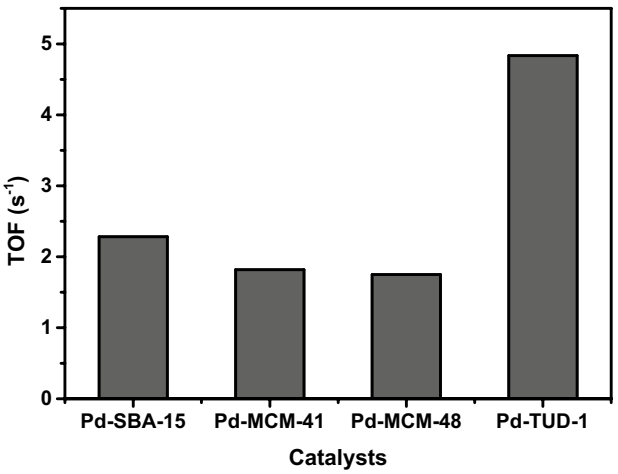

Fig. 7 The calculated TOF of cyclopentene hydrogenation over the four investigated catalysts

test. Figure 8 presents the recycling of Pd-TUD-1 in five cyclopentene hydrogenation runs. The obtained TOF (s^{-1}) is almost the same in the five reactions as an indication for the high stability and reusability of the catalysts. Moreover, leaching test was performed by measuring the amount of Pd in the final liquid product by using ICP technique,

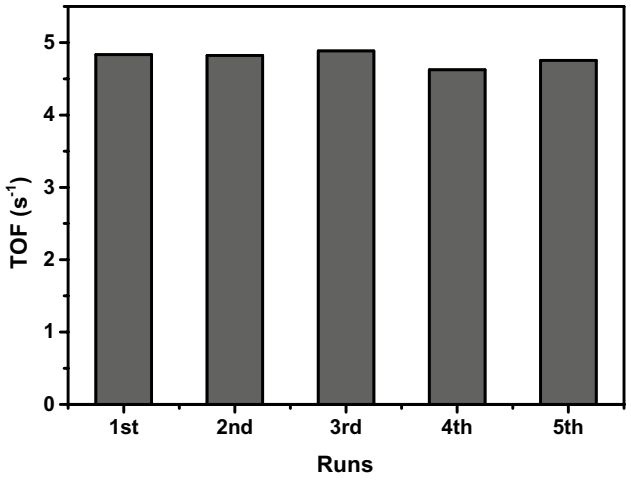

Fig. 8 The TOF (s^{-1}) of the hydrogenation of cyclopentene over Pd-TUD-1 catalyst for five runs

result showed a negligible amount of Pd in the organic phase.

Pd-TUD-1 was proven to be hydrogenated in-situ during the hydrogenation of cyclohexene, and it was reported that in principle the activation of PdO-TUD-1 to be converted to Pd-TUD-1 is not really necessary because Pd^0 nanoparticles are formed in the silica matrix by the hydrogen gas in the cyclohexene organic phase [21]. To confirm the previously obtained results, and XPS investigation was performed for Pd-TUD-1 after five runs to investigate the oxidation state of Pd after the reaction. The obtained results are presented in Fig. 9 and it showed two peaks at 340.9 and 335.5 eV which related to Pd3d3 and Pd3d5, respectively, these two peaks represent the formation of Pd^0 metallic nanoparticles [27, 28].

Moreover, XRD was applied to confirm the formation of Pd^0 active sites in the first few minutes of the reaction in the organic phase of cyclopentene. A hydrogenation reaction was performed as discussed above, however, the reaction was stopped after 3 min and the Pd-TUD-1 was filtrated, washed and dried. Figure 10 shows the XPD patterns of Pd-TUD-1 before and after the 3 min' reaction. It is obviously clear that PdO-TUD-1 is converted to Pd-TUD-1 in the first few minutes of the reaction and therefore, the activation step (the pre-reduction of the catalyst) is not needed in cyclopentene hydrogenation as reported before in cyclohexene hydrogenation. Moreover, HR-TEM study was performed

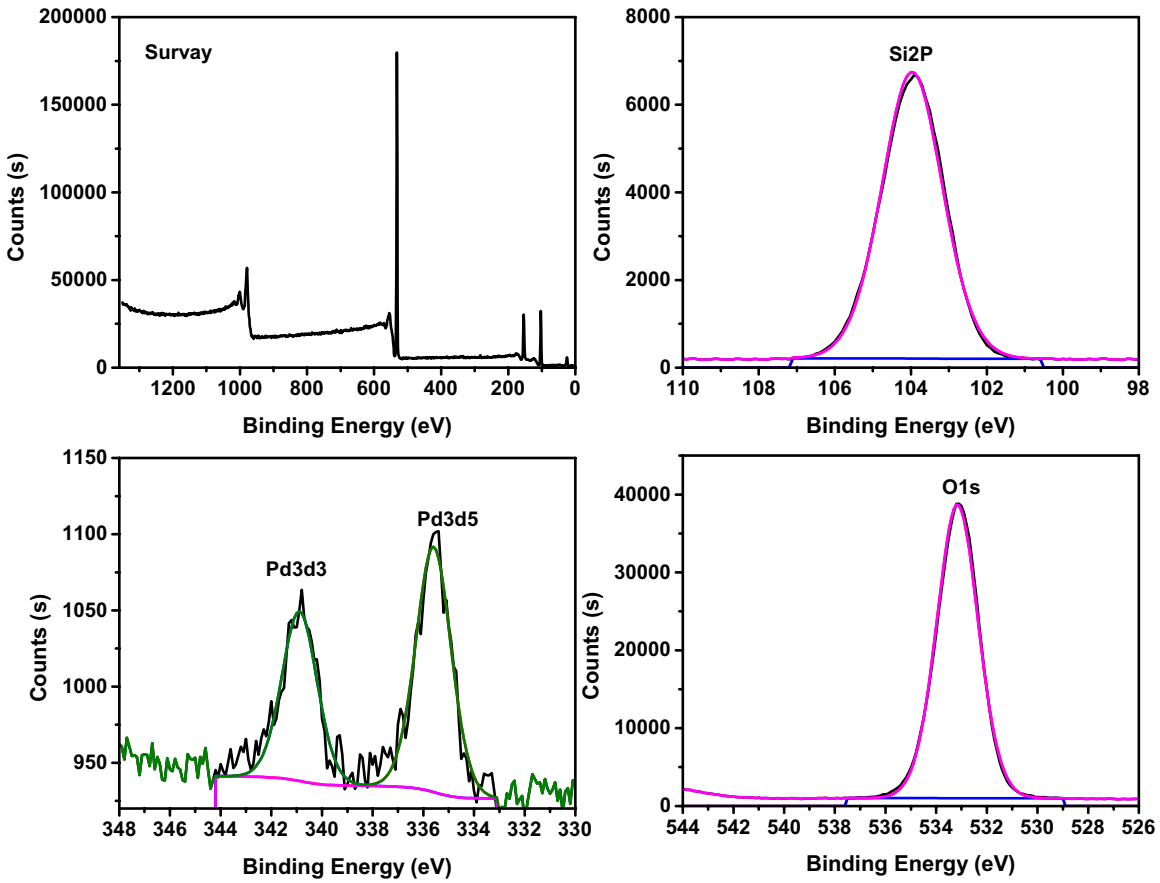

Fig. 9 XPS analysis of Pd-TUD-1 after 5 runs of cyclopentene hydrogenation

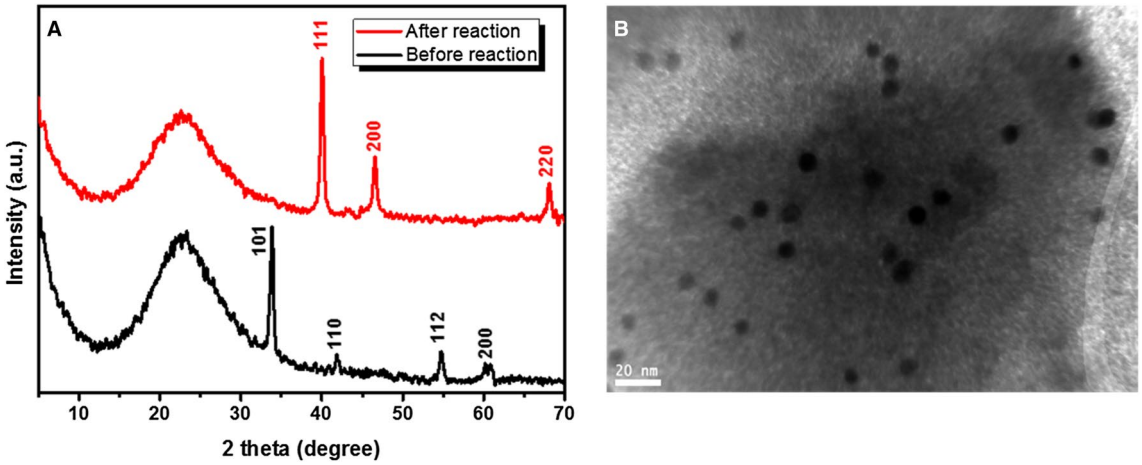

Fig. 10 **a** XRD of Pd-TUD-1 before and after a three minutes' reaction. **b** The HR-TEM micrograph of Pd-TUD-1 sample after a hydrogenation reaction

for Pd-TUD-1 after reaction (Fig. 10b). No severe aggregation or migration could be observed as an indication for the high stability of the Pd nanoparticles supported on TUD-1 mesoporous silica.

4 Discussion

4.1 The difference between the investigated supports

The main differences between the four investigated catalysts can be focused in two points; the amount of Pd active sites and the nature of the support. The TOF number is a fair way to compare the activity between the different catalysts with a normalization of the active sites. Therefore, the nature of the support plays a big role in the obtained activity difference. The differences of the supports' nature can be classified to two main reasons, the morphological structure of each support and its pore system. The four investigate supports are: MCM-41; a 2-D hexagonal uni-dimensional pore system, MCM-48; a 3-D cubic interwoven and continuous 3D pore system, SBA-15; a 2-D hexagonal with a 2-D pore system, and finally; TUD-1, an open structure with an intra-connected 3-D pore system. The open structure 3-D pore system gives an advantage to TUD-1 and MCM-48 for being highly accessible; i.e. the reactants' molecules can easily find the active sites' surfaces and the product's molecules are easily desorb from it. The nature of the pore system plays the reason for why TUD-1 exhibited better performance than MCM-48, the pore volume and pore diameter for TUD-1 is larger than that of MCM-48 which means that TUD-1 pore system does not suffer from the mass transfer limitation, which –most likely- the reason for the less activity of Pd-MCM-48.

In literature, only few articles discussed the effect of support on the behavior of active sites. A comparison between the different mesoporous supports in several applications is listed in Table 2. Six studies out of nine listed studies reported that TUD-1 exhibited the best support for the chosen application.

The reported studies agreed that the three dimensional open pore system of TUD-1 mesoporous material gives a big advantage than the other reported mesoporous materials.

4.2 The proposed mechanism

The mechanism of the cyclopentene hydrogenation catalyzed by supported palladium oxide nanoparticles can be proposed as two main steps: (1) The hydrogenation of PdO to Pd^0 nanoparticles, and (2) The hydrogenation of the double bond. In the first step, the hydrogenation of PdO nanoparticles and the formation of Pd^0 active sites occurs within few seconds even in the liquid organic phase [21]. The more ease diffusion of H_2 gas in the pore system of the mesoporous support to reach the PdO nanoparticle, the faster formation of the required Pd^0 active sites. Here the advantage of the wide pores in the open-structure of TUD-1 makes the differences. This hypothesis can be supported by obtained results, where in the first few minutes of the reaction, almost two times higher conversion was obtained in the case of Pd-TUD-1 compared to other investigated catalysts, this can simply means that the active sites were –most likely– ready faster in the case of TUD-1 (Fig. 11a).

After the formation of Pd^0 active sites, the reaction started as reported in many literature through three main step, 1-adsorption of hydrogen molecules on the solid surface of Pd

Table 2 A comparison between the uses of different mesoporous materials in various applications

Active site	Investigated mesoporous materials	Application	Best performance	References
Blank	TUD-1, SBA-15, MCM-41	Ibuprofen delivery	TUD-1	[29]
Vanadium	TUD-1, SBA-15, MCM-41	isomerization of 1-heptene	SBA-15	[30]
Vanadium	TUD-1, SBA-15, MCM-41	Epoxidation of trans-stilbene and cis-cyclooctene	TUD-1	[31]
Copper	TUD-1, SBA-15, MCM-41, MCM-48	Phenol hydroxylation	TUD-1	[32]
Polyethylenimine	TUD-1, SBA-15	CO_2 capture	TUD-1	[33]
InOx	TUD-1, SBA-15	Baeyer–Villiger oxidation	TUD-1	[34]
Aluminum	TUD-1, SBA-15, MCM-41	Acetalization of glycerol	MCM-41	[35]
Silver	TUD-1, SBA-15, KIT-6	Ethylene/Ethane separation	KIT-6	[36]
Palladium	TUD-1, SBA-15, MCM-41, MCM-48	Hydrogenation of cyclopentene	TUD-1	Current

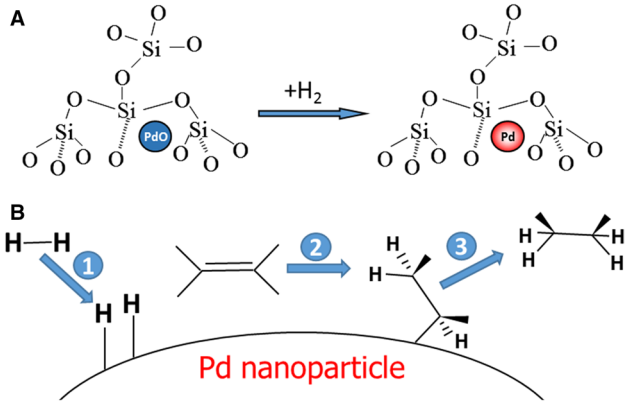

Fig. 11 **a** The first step of the proposed mechanism, the in-situ formation for Pd^0 active sites. **b** The second step of the proposed mechanism, the hydrogenation of cyclopentene to cyclopentane

nanoparticles and dissociate to into hydrogen atoms, 2- one hydrogen is added to one side of the double bond's carbon and the molecules is adsorbed on the Pd surface and finally, c- the second hydrogen atom is added to second carbon of the ex-double bond to form the cyclopentane product which desorbs from the Pd surface. Again, the wide pore system in a three dimensional open structure of TUD-1 offers the maximum accessibility for the reactants to find the Pd^0 active sites and for the product molecules to desorb outside the pore system Fig. 11b).

5 Conclusions

Under the same reaction conditions, 0.5 wt% of Pd was impregnated in four different mesoporous supports; three commercial (MCM-41, MCM-48 and SBA-15) and one home-made (TUD-1). The obtained characterization results confirmed the presence of PdO nanoparticles inside the pores of each mesoporous materials, moreover, elemental analysis showed that SBA-15 was impregnated with the highest Pd amount. The hydrogenation of cyclopentene at room temperature showed that TUD-1 is much active than the other investigated catalysts. This can be explained by the three dimensional open structure in addition to the wide pore system which facilitate the catalytic process.

Acknowledgements The authors are acknowledged the Deanship of Scientific Research at King Khalid University for funding this work through research group program under Grant Number R.G.P.1/115/40. AA, SA and MR extend their appreciation to the Deanship of Scientific Research at King Saud University for funding this work through Research Group, No. RG-1436-005.

References

1. A. Stanislaus, B.H. Cooper, Catal. Rev. **36**, 75 (1994)
2. J.A. Widegren, R.G. Finke, J. Mol. Catal. A **191**, 187 (2003)
3. J.W. Veldsink, M.J. Bouma, N.H. Schöön, A. Beenackers, Catal. Rev. **39**, 253 (1997)
4. L. McEwan, M. Julius, S. Roberts, J. Fletcher, Gold Bull. **43**, 298 (2010)
5. S. Kowalak, R.C. Weiss, K.J. Balkus, J. Chem. Soc. Chem. Commun. **1**, 57 (1991)
6. M. Tada, T. Sasaki, Y. Iwasawa, Phys. Chem. Chem. Phys. **4**, 4561 (2002)
7. M.J. Jacinto, R. Landers, L.M. Rossi, Catal. Commun. **10**, 1971 (2009)
8. V. Caballero, F.M. Bautista, J.M. Campelo, D. Luna, R. Luque, J.M. Marinas, A.A. Romero, J. Mol. Catal. A **308**, 41 (2009)
9. S. Ernst, H. Disteldorf, X. Yang, Microporous Mesoporous Mater. **22**, 457 (1998)
10. P.P. Upare, J.-M. Lee, D.W. Hwang, S.B. Halligudi, Y.K. Hwang, J.-S. Chang, J. Ind. Eng. Chem. **17**, 287 (2011)
11. N.M. Martin, P. Velin, M. Skoglundh, M. Bauer, P.-A. Carlsson, Catal. Sci. Technol. **7**, 1086 (2017)
12. Y.Y. Sun, R. Prins, Angew. Chem. Int. Ed. **47**, 8478 (2008)
13. S. Albertazzi, I. Baraldini, G. Busca, E. Finocchio, M. Lenarda, L. Storaro, A. Talon, A. Vaccari, Appl. Clay Sci. **29**, 224 (2005)
14. L. Chen, R. Luque, Y. Li, Chem. Soc. Rev. **46**, 4614 (2017)
15. C. Xu, R. Fang, R. Luque, L. Chen, Y. Li, Coord. Chem. Rev. **388**, 268 (2019)

16. S. Banerjee, V. Balasanthiran, R.T. Koodali, G.A. Sereda, Org. Biomol. Chem. **8**, 4316 (2010)
17. M. Chatterjee, T. Ishizaka, H. Kawanami, Green Chem. **16**, 4734 (2014)
18. N. Bhorali, J.N. Ganguli, Catal. Lett. **143**, 276 (2013)
19. H. Shen, X. Wu, D. Jiang, X. Li, J. Ni, Chin. J. Catal. **38**, 1597 (2017)
20. M. Benaissa, A.M. Alhanash, M. Eissa, M.S. Hamdy, Catal. Commun. **101**, 62 (2017)
21. A.T. Mubarak, A.M. Alhanash, M. Benaissa, H.H. Hegazy, M.S. Hamdy, Microporous Mesoporous Mater. **278**, 225 (2019)
22. M. Benaissa, A.M. Alhanash, A.T. Mubarak, M. Eissa, T. Sahlabji, M.S. Hamdy, RSC Adv. **8**, 34370 (2018)
23. J.C. Jansen, Z. Shan, L. Marchese, W. Zhou, N. Puil, T. Maschmeyer, Chem. Commun. **8**, 713 (2001)
24. F. Adam, T.-S. Chew, J. Andas, J. Sol-Gel. Sci. Technol. **59**, 580 (2011)
25. S. Ganji, P. Bukya, V. Vakati, K.S.R. Rao, D.R. Burri, Catal. Sci. Technol. **3**, 409 (2013)
26. A. Baylet, P. Marecot, D. Duprez, P. Castellazzi, G. Groppi, P. Forzatti, Phys. Chem. Chem. Phys. **13**, 4607 (2011)
27. P. Concepción, S. García, J.C. Hernández-Garrido, J.J. Calvino, A. Corma, Catal. Today **259**, 213 (2016)
28. T. Hass, J. Gaube, Chem. Eng. Technol. **12**, 45 (1989)
29. T. Heikkilä, J. Salonen, J. Tuura, N. Kumar, T. Salmi, D. Yu Murzin, M.S. Hamdy, G. Mul, L. Laitinen, A.M. Kaukonen, J. Hirvonen, V.-P. Lehto, Drug Deliv. **14**, 337 (2007)
30. S. Hu, D. Liu, L. Li, Z. Guo, Y. Chen, A. Borgna, Y. Yang, Chem. Eng. J. **165**, 916 (2010)
31. Z. Guo, C. Zhou, S. Hu, Y. Chen, X. Jia, R. Lau, Y. Yang, Appl. Catal. A **419**, 194 (2012)
32. M.P. Pachamuthu, V.V. Srinivasan, R. Maheswari, K. Shanthi, A. Ramanathan, Catal. Sci. Technol. **3**, 3335 (2013)
33. X. Wang, C. Song, A.M. Gaffney, R. Song, Catal. Today **238**, 95 (2014)
34. R. Kumar, P.P. Das, A.S. Al-Fatesh, A.H. Fakeeha, J.K. Pandey, B. Chowdhury, Catal. Commun. **74**, 80 (2016)
35. P. Manjunathan, V.S. Marakatti, P. Chandra, A.B. Kulal, S.B. Umbarkar, R. Ravishankar, G.V. Shanbhag, Catal. Today **309**, 61 (2018)
36. C. Wu, J. Wang, Y. Fang, Z. Wang, D. Fei, X. Han, Y. Dang, J. Chem. Eng. Data **64**, 611 (2019)